

Laser damage creates backdoors in quantum communications

Vadim Makarov,^{1,2,3,4,a)} Jean-Philippe Bourgoin,^{2,3} Poompong Chaiwongkhot,^{2,3} Mathieu Gagné,⁵ Thomas Jennewein,^{2,3,6} Sarah Kaiser,^{2,3} Raman Kashyap,⁵ Matthieu Legré,⁷ Carter Minshull,² and Shihan Sajeed^{2,4}

¹⁾*The rest of the authors are listed alphabetically.*

²⁾*Institute for Quantum Computing, University of Waterloo, Waterloo, ON, N2L 3G1 Canada*

³⁾*Department of Physics and Astronomy, University of Waterloo, Waterloo, ON, N2L 3G1 Canada*

⁴⁾*Department of Electrical and Computer Engineering, University of Waterloo, Waterloo, ON, N2L 3G1 Canada*

⁵⁾*Department of Engineering Physics and Department of Electrical Engineering, École Polytechnique de Montréal, Montréal, QC, H3C 3A7 Canada*

⁶⁾*Quantum Information Science Program, Canadian Institute for Advanced Research, Toronto, ON, M5G 1Z8 Canada*

⁷⁾*ID Quantique SA, Chemin de la Marbrerie 3, 1227 Carouge, Geneva, Switzerland*

(Dated: 12 October 2015)

Quantum communication protocols such as quantum cloud computing¹, digital signatures², coin-tossing³, secret-sharing⁴, and key distribution⁵, using similar optical technologies, claim to provide unconditional security guaranteed by quantum mechanics. Among these protocols, the security of quantum key distribution (QKD) is most scrutinized and believed to be guaranteed as long as implemented devices are properly characterized and existing implementation loopholes are identified and patched^{6,7}. Here we show that this assumption is not true. We experimentally demonstrate a class of attacks based on laser damage⁸, capable of creating new security loopholes on-demand. We perform it on two different implementations of QKD and coin-tossing protocols, and create new information leakage side-channels. Our results show that quantum communication protocols cannot guarantee security alone, but will always have to be supported by additional technical countermeasures against laser damage.

Cryptography, an art of secure communication, has traditionally relied on either algorithmic or computational complexity⁹. Even the most state-of-the-art classical cryptographic schemes do not have a strict mathematical proof to ascertain their security. With the advance of quantum computing, it may be a matter of time before the security of the most widely used public-key cryptography protocols is broken¹⁰. However, QKD (popularly known as quantum cryptography)⁵ allows remote key distribution with unconditional security^{6,7}. Its complete security model is based on the laws of quantum mechanics, security proofs and model of equipment. When we go from theory to practice, the practical behaviour of the implemented equipment often deviates from its modeled behaviour, leading to a compromise of security^{11–16}. However, it is widely assumed that as long as these deviations are properly characterized and security proofs are updated accordingly^{7,17}, QKD can provide unconditional security. In this work we show that this is not always true for QKD and other secure

quantum communication protocols. Even if a system is perfectly characterized and deviations are included into the security proofs, an eavesdropper can still create a new deviation on-demand, unlike in classical cryptography schemes.

The reason behind this is that in classical communication systems, the security-critical parts can be physically separated from the communication channel, thus making them isolated from physical access and alteration by the eavesdropper¹⁸. However, the front-end of a quantum communication system is essentially an analog optical system connected to the channel, and easily accessible by an eavesdropper. The latter may shoot a high-power laser from the communication channel to damage a security-critical component of the system, rendering the system insecure⁸. To verify this possibility, we perform laser damage on two completely different widely used implementations: a commercial fiber-optic system for QKD and coin-tossing with phase-encoded qubits^{19,20}, and a free-space system for QKD with polarization-encoded qubits²¹. In both systems, the damage opens up a new side-channel, which can compromise the security of QKD even with today's technology^{16,22}.

Although we have only tested implementations of QKD and coin-tossing, the security of other quantum communication protocols seems to rely on broadly similar assumptions, and they use similar optical technology. For example, in quantum cloud computing¹ and digital signatures², client's and Alice's state preparation may be eavesdropped on. Quantum implementations of oblivious transfer²³ and relativistic bit commitment²⁴ are based on modified QKD setups and thus suffer from the same vulnerabilities. However the implementations and security criteria of those protocols are less developed, making their battle-testing a future task.

Laser damage in fiber-optic quantum communication system. To demonstrate the threat of laser damage in a fiber-optic quantum communication implementation, we chose a plug-and-play QKD¹⁹ and loss-tolerant quantum coin tossing (QCT)³. Both were implemented using a commercial system Clavis2 from ID Quantique²⁰. In both cases, Bob sends bright light pulses to Alice. Alice randomly encodes her secret bits

^{a)}Electronic mail: makarov@vad1.com

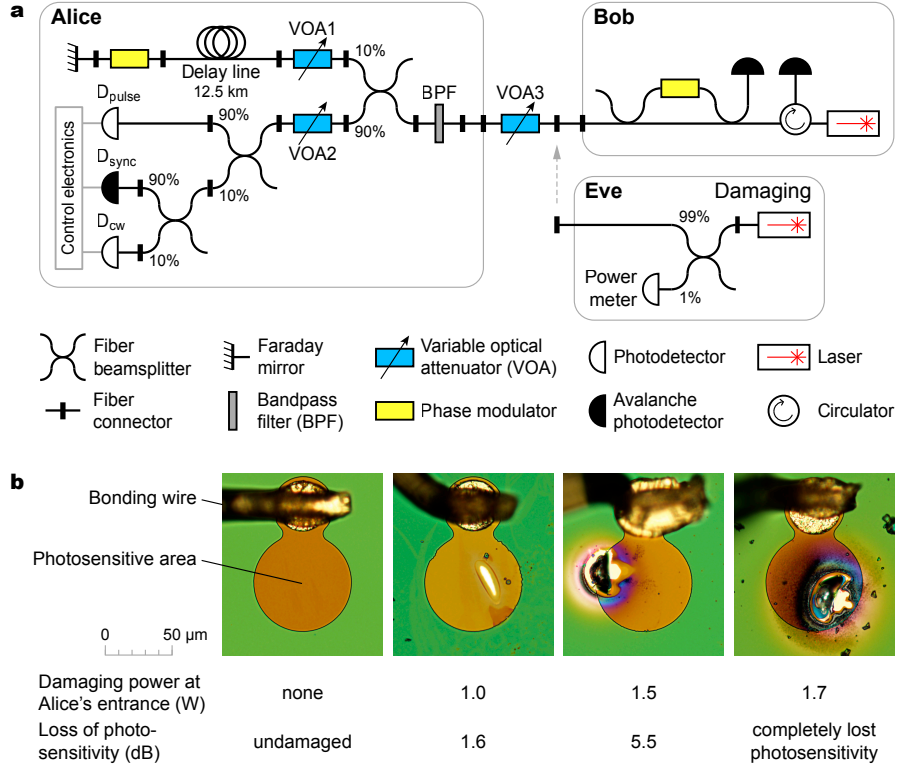


FIG. 1. Attack on fiber-optic system Clavis2. **a**, Experimental setup. The system consists of Alice and Bob connected by a lossy fiber communication channel (simulated by variable optical attenuator VOA3). Bob sends to Alice pairs of bright coherent optical pulses, produced by his laser and two fiber arms of unequal length^{19,20}. Alice uses fiber beamsplitters to divert parts of incoming pulse energy to monitoring detector D_{pulse} , synchronization detector D_{sync} and line-loss measurement detector D_{cw} . She prepares quantum states by phase-modulating the pulses, reflecting them at a Faraday mirror and attenuating to single-photon level with VOA1. Bob measures the quantum states by applying his basis choice via phase modulator and detecting outcome of quantum interference with single-photon avalanche photodetectors. Eve's damaging laser is connected to the channel manually. BPF, bandpass filter. **b**, Pulse-energy-monitoring photodiode before and after damage. Brightfield microphotographs show top-view of decapsulated photodiode chips. The last two samples have holes melted through their photosensitive area. Scattered dark specks are debris from decapsulation.

by applying one out of four phases ($0, \frac{\pi}{2}, \pi, \frac{3\pi}{2}$), attenuates the pulses and reflects them back to Bob (Fig. 1a). The security of both protocols requires an upper bound on the mean photon number μ coming out of Alice. Otherwise, an eavesdropper Eve can perform a Trojan-horse attack²⁵ by superimposing extra light to the bright pulses on their way to Alice from Bob. If Alice is unaware of this and applies the same attenuation, then light coming out of her has a higher μ than allowed by the security proofs⁷, making the implementations insecure. It is thus crucial for the security of both protocols that Alice monitors the incoming pulse energy. This is achieved by employing a pulse-energy-monitoring detector (D_{pulse} in Fig. 1a). A portion of the incoming light is fed to D_{pulse} such that whenever extra energy is injected, an alarm is produced²². The sensitivity of D_{pulse} is factory-calibrated, thus closing the side-channel associated with the Trojan-horse attack.

We tested the endurance of this countermeasure against laser damage. During normal QKD operation, we disconnected the fiber channel Alice–Bob temporarily and connected Eve (Fig. 1a). She then injected 1550 nm laser light from an erbium-doped fiber amplifier for 20–30 s, delivering continuous-wave (c.w.) high power into Alice's entrance. 44%

of this power reached the fiber-pigtailed InGaAs p-i-n photodiode D_{pulse} (JDSU EPM 605LL), and damaged it partially or fully. It became either less sensitive to incoming light (by 1–6 dB after 0.5–1.5 W illumination at Alice's entrance) or completely insensitive (after ≥ 1.7 W). The physical damage is shown in Fig. 1b. No other optical component was damaged. We repeated the experiment with 6 photodiode samples. In half of these trials, QKD continued uninterrupted after we reconnected the channel back to Bob, as if nothing has happened. In the other half, a manual software restart was needed. However, in all the trials the damage was sufficient to permanently open the system up to the Trojan-horse attack. As modeled in Ref. 22, in the QKD protocol, Eve can eavesdrop partial or full key using today's best technology if the sensitivity of D_{pulse} drops by more than 5.6 dB. In the QCT implementation, a sensitivity reduction by 2.6 dB can increase Bob's cheating probability above a classical level, removing any quantum advantage of coin-tossing. Laser damage thus compromises both the QKD and QCT implementations. See Methods for details.

Laser damage in free-space quantum communication system. As a representative of free-space quantum communi-

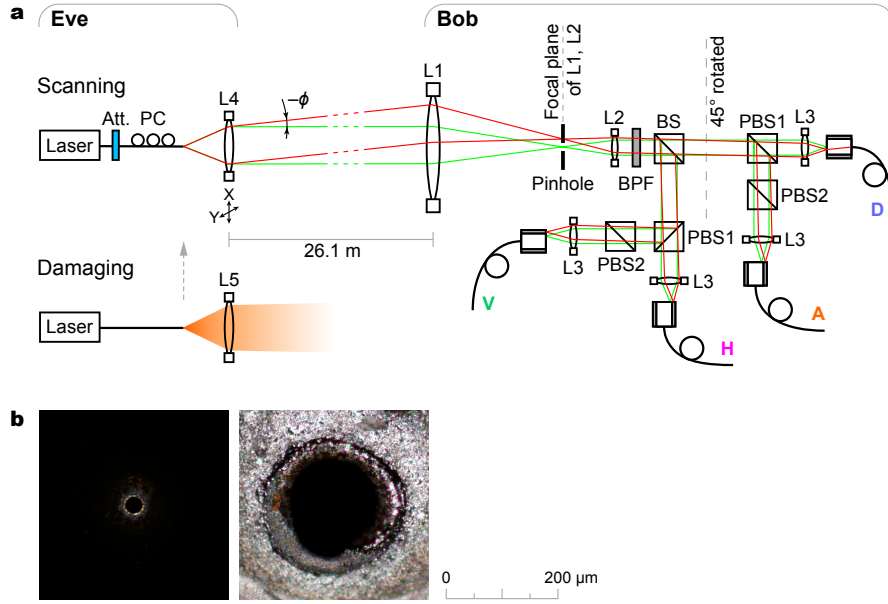


FIG. 2. Attack on free-space QKD system. **a**, Experimental setup. QKD receiver Bob consists of two lenses L1, L2 reducing input beam diameter, 50:50 beamsplitter BS, and two arms measuring photons in HV and DA polarizations using polarizing beamsplitters PBS^{16,21}. Photons are focused by lenses L3 into multimode fibers leading to single-photon detectors. Setup drawing is not to scale. Eve’s apparatus contains a scanning laser source that tilts the beam angle (ϕ, θ) by laterally shifting lens L4. Green marginal rays denote initial Eve’s alignment, replicating the alignment Alice–Bob at $\phi = \theta = 0$. Red marginal rays show a tilted scanning beam missing fiber cores V, H, A, but coupling into D. Eve’s damaging laser source can be manually inserted in place of the scanning source. Att., attenuator; PC, polarization controller. **b**, Spatial filter before and after damage. Darkfield microphotographs show front view of the pinhole. See Supplementary Video 1 for real-time recording of laser damage to the pinhole inside Bob.

cation, we chose a long-distance satellite QKD prototype operating at 532 nm wavelength²¹ employing Bennett-Brassard 1984 (BB84) protocol⁵. At each time slot, Alice randomly sends one out of four polarizations: horizontal (H), vertical (V), $+45^\circ$ (D), or -45° (A) using a phase-randomized attenuated laser. Bob randomly measures in either horizontal-vertical (HV) or diagonal-antidiagonal (DA) basis, using a polarization-beamsplitter receiver (Fig. 2a). It has been shown in Ref. 16 that an eavesdropper can, in practice, tilt the beam going towards Bob by an angle (ϕ, θ) such that the beam misses, partially or fully, the cores of fibers leading to three detectors while being relatively well coupled into the core leading to the fourth detector, as illustrated in Fig. 2a. This happens because real-world optical alignments are inherently imperfect and manufacturing precision is finite. By sending light at different spatial angles, the eavesdropper can have control over Bob’s basis and measurement outcome and steal the key unnoticed^{14,16,26}. This attack can be prevented by placing a spatial filter or ‘pinhole’ at the focal plane of lenses L1 and L2, as shown in Fig. 2a¹⁶. Since the pinhole limits the field of view, any light entering at a higher spatial angle is blocked and Eve no longer has access to the target angles required to have control over Bob. As was demonstrated in Ref. 16, a pinhole of 25 μm diameter eliminates this side-channel by making the angular efficiency dependence identical between the four detectors (Fig. 3a).

We tested the endurance of this countermeasure against laser damage. From a distance of 26.1 m, we shot an 810 nm

collimated laser beam delivering a 10 s pulse of 3.6 W c.w. power at the pinhole inside Bob’s setup. The intensity there was sufficient to melt the material (13 μm thick stainless steel) and enlarge the hole diameter to $\approx 150 \mu\text{m}$. The state of the pinhole before and after damage is shown in Fig. 2b, and the damage process in real time is shown in Supplementary Video 1. Although Bob was up and running in photon counting mode during the test, none of his other components were damaged. See Methods for experimental details.

With this larger pinhole opening, it was again possible to send light at angles that had relatively higher mismatches in efficiency, as shown in Fig. 3b. This enabled a faked-state attack under realistic conditions of channel loss in 1–15 dB range with quantum bit error ratio (QBER) $< 6.6\%$ (see Methods). Thus laser damage completely neutralizes this countermeasure, and makes this free-space QKD system insecure.

Discussion. The crucial step of the attack, creating the loophole, has thus been experimentally demonstrated for both systems tested. After this, building a complete eavesdropper would be a realistic if time-consuming task²⁷.

Countermeasures to the laser-damage attack may include a passive optical power limiter²⁸, a single-use ‘fuse’ that permanently breaks the optical connection if a certain power is exceeded, or battery-powered active monitoring supplemented with wavelength filtering. Hardware self-characterization may be promising²⁹, however to protect from an arbitrary damage it must monitor a potentially large number of hardware parameters. Any countermeasure must be tested in all

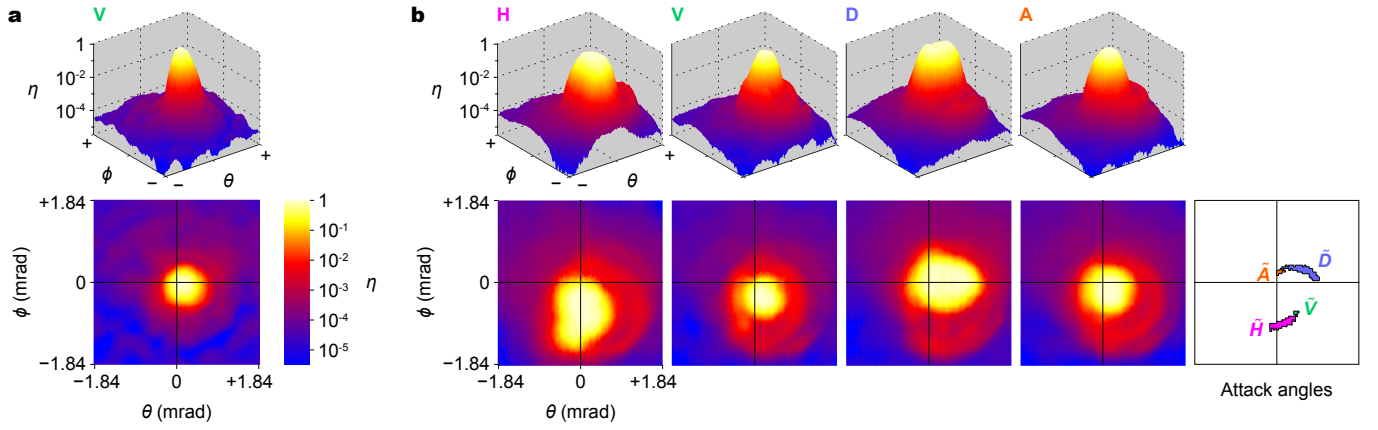


FIG. 3. **Efficiency-mismatch side-channel opened after laser damage in free-space QKD system.** Each pair of 3D–2D plots shows normalised photon detection efficiency η in a receiver channel versus illuminating beam angles ϕ and θ . **a**, Before laser damage, the angular dependence is essentially identical between the four channels¹⁶. Plot for one channel (V) before damage is shown. **b**, After the laser damage, the four receiver channels H, V, D, A exhibit unequal sensitivity to photons outside the middle area around $\phi = \theta = 0$. The last plot shows angular ranges for targeting the four detectors that satisfy conditions for the faked-state attack.

possible illumination regimes. Eve can use a wide range of wavelengths and optical pulse durations. Optical fiber transmits wavelengths from ultraviolet to ~ 2000 nm, while free-space optics may also be transparent at longer wavelengths. While we have demonstrated c.w. thermal laser damage on the timescale of seconds, short-pulsed laser radiation may induce different damage mechanisms³⁰. Furthermore, systems can be attacked in both powered and unpowered state (e.g., during an outage or maintenance). By Kerckhoffs' principle³¹, Eve is assumed to predict and know the damage precisely. In practice when attacking installed systems, she may characterize them by imaging, reflectometry²⁵ and watching public communication Alice–Bob while probing their response to attack sporadically, adjusting her attack parameters until they enable full eavesdropping²⁶. In summary, construction of counter-measures that guarantee security remains an open question.

In this work we have tested two QKD systems and a QCT system against laser damage, and compromised the security of each. Although we have not experimentally tested this, it seems the security parameters, characteristics and assumptions of any other implementations of quantum communication protocols might also be vulnerable to laser damage. For example, in a coherent-one-way QKD scheme³², the front-end contains an attenuator, coupler, and monitoring p-i-n detector, all of which are potentially vulnerable. Similarly, there is no guarantee that the measurement-device-independent³³ and fully-device-independent³⁴ QKD implementations cannot be altered by laser damage (potentially breaking the assumptions of a trusted source in the former and the absence of information-leakage channels in the latter). Any alteration of characteristics might compromise the security either directly by leading to an attack, or indirectly by shifting some parameter in the security proof so it would no longer apply. Since the laser damage is a new eavesdropping tool that alters a well-characterized system, the community needs to think again how to ascertain the security proofs against changing security parameters. We expect that testing against optical attacks

including laser damage will become an obligatory part of security assurance for future quantum communications.

- ¹Barz, S. *et al.* Demonstration of blind quantum computing. *Science* **335** 303–308 (2012).
- ²Collins, R. J. *et al.* Realization of quantum digital signatures without the requirement of quantum memory. *Phys. Rev. Lett.* **113** 040502 (2014).
- ³Pappa, A. *et al.* Experimental plug and play quantum coin flipping. *Nat. Commun.* **5** 3717 (2014).
- ⁴Grice, W. P. *et al.* Two-party secret key distribution via a modified quantum secret sharing protocol. *Opt. Express* **23** 7300 (2015).
- ⁵Bennett, C. H. & Brassard, G. Quantum Cryptography: Public Key Distribution and Coin Tossing. In *Proceedings of IEEE International Conference on Computers, Systems, and Signal Processing*, 175–179 (IEEE Press, New York, Bangalore, India, 1984).
- ⁶Lo, H.-K. & Chau, H. F. Unconditional security of quantum key distribution over arbitrarily long distances. *Science* **283** 2050–2056 (1999).
- ⁷Gottesman, D., Lo, H.-K., Lütkenhaus, N. & Preskill, J. Security of quantum key distribution with imperfect devices. *Quant. Inf. Comp.* **4** 325–360 (2004).
- ⁸Bugge, A. N. *et al.* Laser damage helps the eavesdropper in quantum cryptography. *Phys. Rev. Lett.* **112** 070503 (2014).
- ⁹Singh, S. *The Code Book: The Science of Secrecy from Ancient Egypt to Quantum Cryptography* (Fourth Estate, London, 1999).
- ¹⁰Shor, P. W. Polynomial-time algorithms for prime factorization and discrete logarithms on a quantum computer. *SIAM J. Comput.* **26** 1484–1509 (1997).
- ¹¹Bennett, C. H., Bessette, F., Salvail, L., Brassard, G. & Smolin, J. Experimental quantum cryptography. *J. Cryptology* **5** 3–28 (1992).
- ¹²Makarov, V., Anisimov, A. & Skaar, J. Effects of detector efficiency mismatch on security of quantum cryptosystems.

- Phys. Rev. A* **74** 022313 (2006). Erratum *ibid.* **78**, 019905 (2008).
- ¹³Qi, B., Fung, C.-H. F., Lo, H.-K. & Ma, X. Time-shift attack in practical quantum cryptosystems. *Quant. Inf. Comp.* **7** 73–82 (2007).
 - ¹⁴Lydersen, L. *et al.* Hacking commercial quantum cryptography systems by tailored bright illumination. *Nat. Photonics* **4** 686–689 (2010).
 - ¹⁵Sun, S.-H., Jiang, M.-S. & Liang, L.-M. Passive Faraday-mirror attack in a practical two-way quantum-key-distribution system. *Phys. Rev. A* **83** 062331 (2011).
 - ¹⁶Sajeed, S. *et al.* Security loophole in free-space quantum key distribution due to spatial-mode detector-efficiency mismatch. *Phys. Rev. A* **91** 062301 (2015).
 - ¹⁷Fung, C.-H. F., Tamaki, K., Qi, B., Lo, H.-K. & Ma, X. Security proof of quantum key distribution with detection efficiency mismatch. *Quant. Inf. Comp.* **9** 131–165 (2009).
 - ¹⁸*National security telecommunications and information systems security advisory memorandum (NSTISSAM) TEMPEST/2-95, red/black installation guidance* (US National Security Agency, 1995). Declassified in 2000. <http://cryptome.org/tempest-2-95.htm>.
 - ¹⁹Stucki, D., Gisin, N., Guinnard, O., Ribordy, G. & Zbinden, H. Quantum key distribution over 67 km with a plug&play system. *New J. Phys.* **4** 41–41 (2002).
 - ²⁰Clavis2 specification sheet, <http://www.idquantique.com/images/stories/PDF/clavis2-quantum-key-distribution/clavis2-specs.pdf>, visited 27 July 2015.
 - ²¹Bourgoin, J.-P. *et al.* Experimentally simulating quantum key distribution with ground-to-satellite channel losses and processing limitations (manuscript in preparation).
 - ²²Sajeed, S. *et al.* Attacks exploiting deviation of mean photon number in quantum key distribution and coin tossing. *Phys. Rev. A* **91** 032326 (2015).
 - ²³Erven, C. *et al.* An experimental implementation of oblivious transfer in the noisy storage model. *Nat. Commun.* **5** 3418 (2014).
 - ²⁴Lunghi, T. *et al.* Experimental bit commitment based on quantum communication and special relativity. *Phys. Rev. Lett.* **111** 180504 (2013).
 - ²⁵Vakhitov, A., Makarov, V. & Hjelme, D. R. Large pulse attack as a method of conventional optical eavesdropping in quantum cryptography. *J. Mod. Opt.* **48** 2023–2038 (2001).
 - ²⁶Makarov, V. & Hjelme, D. R. Faked states attack on quantum cryptosystems. *J. Mod. Opt.* **52** 691–705 (2005).
 - ²⁷Gerhardt, I. *et al.* Full-field implementation of a perfect eavesdropper on a quantum cryptography system. *Nat. Commun.* **2** 349 (2011).
 - ²⁸Tutt, L. W. & Boggess, T. F. A review of optical limiting mechanisms and devices using organics, fullerenes, semiconductors and other materials. *Prog. Quant. Electr.* **17** 299–338 (1993).
 - ²⁹Lydersen, L., Makarov, V. & Skaar, J. Secure gated detection scheme for quantum cryptography. *Phys. Rev. A* **83** 032306 (2011).
 - ³⁰Wood, R. M. *Laser-Induced Damage of Optical Materials* (CRC Press, 2003).
 - ³¹Kerckhoffs, A. La cryptographie militaire. *J. des Sciences Militaires* **IX** 5–38 (1883).
 - ³²Walenta, N. *et al.* A fast and versatile quantum key distribution system with hardware key distillation and wavelength multiplexing. *New J. Phys.* **16** 013047 (2014).
 - ³³Lo, H.-K., Curty, M. & Qi, B. Measurement-device-independent quantum key distribution. *Phys. Rev. Lett.* **108** 130503 (2012).
 - ³⁴Acín, A., Gisin, N. & Masanes, L. From Bell’s theorem to secure quantum key distribution. *Phys. Rev. Lett.* **97** 120405 (2006).
 - ³⁵Jain, N. *et al.* Device calibration impacts security of quantum key distribution. *Phys. Rev. Lett.* **107** 110501 (2011).
 - ³⁶Stucki, D. *et al.* Long-term performance of the SwissQuantum quantum key distribution network in a field environment. *New J. Phys.* **13** 123001 (2011).
 - ³⁷Sauge, S., Lydersen, L., Anisimov, A., Skaar, J. & Makarov, V. Controlling an actively-quenched single photon detector with bright light. *Opt. Express* **19** 23590–23600 (2011).

Acknowledgements. We thank Q. Liu, E. Anisimova and O. Di Matteo for early experimental efforts, S. Todoroki, N. Lütkenhaus, M. Mosca, Y. Zhang and L. Lydersen for discussions. This work was supported by the US Office of Naval Research, Industry Canada, CFI, Ontario MRI, NSERC, Canadian Space Agency, ID Quantique, European Commission’s FET QICT SIQS project, EMPIR 14IND05 MIQC2 project, and CryptoWorks21. We acknowledge using University of Waterloo’s Quantum NanoFab. P.C. was supported from Thai DPST scholarship. J.-P.B. was supported by FED DEV.

Conflicts of interest. A part of this study was supported and M.L. was employed by ID Quantique. The company has been informed prior to this publication, and is developing countermeasures for their affected QKD system. The other authors declare no competing financial interests.

Author contributions. V.M. conceived and led the study. S.K. implemented the fiber-optic experiment. S.S. implemented the free-space experiment and contributed to the fiber-optic experiment. P.C. contributed to the free-space experiment. M.G. contributed to the fiber-optic experiment. C.M. made minor contributions to the free-space experiment. M.L. provided and supported the fiber-optic QKD system under test. T.J. and J.-P.B. provided the free-space QKD receiver under test and contributed to the free-space experiment. R.K. provided the fiber laser facility and co-supervised the fiber-optic experiment. S.S. and V.M. wrote the article, with contributions from all authors.

METHODS

Laser-damage experiment on fiber-optic system. In our experiment, we damaged D_{pulse} during QKD operation, trying not to interrupt it. The system was allowed to start up and produce a secret key for several QKD cycles, using BB84 protocol⁵. To perform laser damage, we disconnected the channel for 2–3 min, giving us enough time to apply high power to Alice, and then reconnected the channel. We tried this at different points in the QKD operation cycle. Sometimes the software recovered and resumed QKD, and sometimes it got stuck in recalibration routines. In the latter case, a manual software restart resumed QKD. Owing to a limited number of trials, we did not perfect this timing aspect.

We tested a total of 6 photodiode samples. We damaged each of them by applying high power laser light at Alice’s entrance. We then used the manufacturer’s factory-calibration software to measure how much extra signal power (compared to the pre-calibrated power level) could be injected without triggering the alarm²². This quantified the reduction in sensitivity due to the damage. Three samples were exposed twice to a progressively higher power. For example, one sample was first exposed to 0.5 W power at Alice’s entrance that reduced its photosensitivity by 1 dB, then to 0.75 W power that reduced its photosensitivity by 6 dB. For the other two samples these numbers were 0.75 W with no change in sensitivity then 1.0 W, 1.6 dB (shown in 2nd microphotograph in Fig. 1b); 1.0 W, 5 dB then 1.5 W, 5.5 dB (shown in 3rd microphotograph in Fig. 1b). For the remaining three samples, 1.7 W was applied at Alice’s entrance, and D_{pulse} completely lost photosensitivity, becoming electrically either a large resistor (shown in 4th microphotograph in Fig. 1b) or an open circuit. After we were done with each sample, we used the same manufacturer’s factory-calibration software to pre-calibrate the sensitivity of the next undamaged D_{pulse} sample, following the factory procedure.

No other component in Alice was damaged during these trials. We also tested some components separately. FC/PC and FC/APC optical connectors used in Alice and in the channel withstood 3 W c.w., while copies of Alice’s 10:90 fiber beam-splitters (AFW Technologies FOSC-1-15-10-L-1-S-2) withstood up to 8 W c.w. with no damage.

Figure 4 summarizes a system operation log when it recovered automatically after the damage that made the photodiode an open-circuit with no photosensitivity. In the current system implementation, this represents an ideal outcome for an attacker.

For damaging and component tests, Eve used an erbium-doped fiber amplifier seeded from a 1550.7 nm laser source (EDFA; IPG Photonics ELR-70-1550-LP). She injected 0–2 W c.w. power at Alice’s entrance. The injected power was monitored with a 1:99 fiber beamsplitter tap and a power meter (Fig. 1a). A manually operated shutter at the output of EDFA allowed to ramp the power up and down smoothly between 0 and the target level, with tens of milliseconds transition time. The spectral characteristics of EDFA’s built-in seed laser did not precisely match the passband of the BPF at Alice’s entrance (1551.32–1552.12 nm passband at -0.5 dB

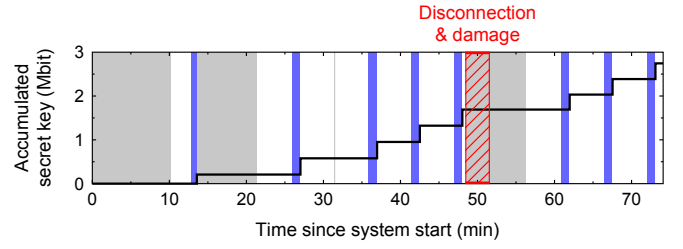


FIG. 4. Fiber-optic QKD system operation during laser damage. The plot shows accumulated secret key amount versus time. Grey bands denote the system performing recalibration routines, white bands denote the quantum bit sending and receiving, and blue (darker) bands denote classical post-processing. All this information was extracted from the QKD system log files after the experiment. The band hatched in red denotes the time when the fiber channel Alice–Bob was temporarily disconnected and the laser damage to Alice was done by 1.7 W laser power, resulting in D_{pulse} becoming an open circuit with no photosensitivity.

level, < 0.7 dB insertion loss; AFW Technologies BPF-1551.72-2-B-1-1). We therefore removed the BPF for the duration of experiment. The BPF was separately tested in-passband using a different EDFA (PriTel LNHPFA-37) with a narrowband seed laser, and passed more than 1 W c.w. with no damage.

The system QKD software (‘QKD Sequence’ application²⁰) set the variable attenuator VOA2 at 2 dB. Thus, 44% of Alice’s incoming light impinged D_{pulse} , while smaller fractions impinged D_{sync} and D_{cw} . The alarm threshold of D_{pulse} is calibrated when the system is assembled at the factory, and is not changed after that²². VOA3 introduced channel loss of 1.87 dB, to simulate the effect of ≈ 9 km long fiber line Alice–Bob.

The QKD system Clavis2 normally operates automatically in cycles consisting of sending and receiving quantum states until either the memory buffer is full or photon detection efficiency has dropped significantly. It then uses the classical link Alice–Bob to post-process the detected data and distill the secret key¹¹. Each cycle takes several minutes. If the last QKD cycle was interrupted because the detection efficiency was too low, or the key distillation failed, the system returns to start-up routines such as timing recalibration³⁵ before it resumes sending quantum states. This happens often in normal operation, because of naturally occurring drift of hardware and channel parameters. The software generally tries to recover automatically from various error conditions, to provide long-term unattended operation³⁶.

Predicted attacks on fiber-optic system with damaged pulse-energy-monitoring photodiode. As modeled in Ref. 22, for BB84 QKD protocol Eve can eavesdrop partial or full key information using today’s best photonics technologies when the sensitivity of D_{pulse} has dropped by 4.3–5.6 dB, given that communication channel loss Alice–Bob is in a 1–7 dB range. (This corresponds to a multiplication factor x in the range of 2.7–3.6, see Fig. 11 in Ref. 22.) If we assume that Eve’s equipment is only limited by the laws of quantum mechanics, then she can extract the full key information after

only 0.4–0.8 dB reduction in sensitivity (x of 1.1–1.2). Similarly, for QCT with a dishonest Bob only limited by the quantum mechanics, all the quantum advantages of the protocol are eliminated if sensitivity reduction of 2.6 dB is obtained in Alice ($x = 1.805$), for a 15 km long communication channel. For a 10 dB sensitivity reduction, Bob’s cheating probability approaches unity²². Since we have surpassed the above sensitivity reduction thresholds in our laser damage experiment, we consider the security of both QKD and QCT implementation compromised.

Laser-damage experiment on free-space QKD system. In order to neutralize the effect of the pinhole and reproduce the side-channel of spatial-mode detector-efficiency mismatch, our experiment consisted of three steps. Firstly, we performed scanning to certify that the system is secure against this side-channel. Secondly, we laser-damaged the pinhole to open the side-channel. Finally, we performed scanning again to demonstrate that the system’s security has been compromised. In all three steps, Eve was placed at a distance of 26.1 m away from Bob and the steps were performed in sequence without making any interactions with Bob.

The first step involved changing the outgoing beam’s angle (ϕ, θ) emitted from Eve’s scanning setup shown in Fig. 2a, then recording the corresponding count rate at all four detectors in Bob. This step is identical to that in Ref. 16. The scanning result is shown in Fig. 3a, where a pair of 3D–2D plots shows the normalized photon detection efficiency in one receiver channel versus the illuminating beam angles ϕ and θ . With the pinhole in place, the angular dependence of efficiency is essentially identical between the four channels, hence only a plot for channel V is shown. No measurable amount of efficiency mismatch was found and no attack angles existed¹⁶.

Then as the second step, Eve’s scanning setup was replaced with the damaging setup. The latter contained a 810 nm laser diode (Jenoptik JOLD-30-FC-12) pumped by a current-stabilized power supply and connected to 200 μ m core diameter multimode fiber. It provided continuously adjustable 0 to 30 W c.w. power into the fiber. An almost-collimated free-space beam was subsequently formed by a plano-convex lens L5 (Thorlabs LA1131-B; Fig. 2a). The beam’s intensity was nearly uniformly distributed across Bob’s L1 (50 mm diameter achromatic doublet, Thorlabs AC508-250-A), with less than $\pm 10\%$ intensity fluctuation across Bob’s input aperture. Transmission of L1 was about 82%, owing to its antireflection coating being designed for a different wavelength band. In the test detailed here, the power delivered at the pinhole plane was 3.6 W, sufficient to reliably produce a hole of ≈ 150 μ m diameter in less than 10 s in a standard stainless-steel foil pinhole (Thorlabs P25S). We also tested that power decreased to 2.0 W still produced a hole. No other component in Bob was damaged during the tests. Bob’s lenses L4 received ~ 1 μ W power each, and single-photon detectors only received on the order of a few nW each, mainly owing to the presence of BPF after the pinhole. The BPF was used by Bob to increase the signal-to-noise ratio during QKD by heavily attenuating all light outside the 531–533 nm passband (it consisted of two stacked filters, Thorlabs FESH0700 followed by Semrock

LL01-532-12-5)²¹. While the damaging beam was on, the detectors counted at their saturation rate of ~ 35 MHz, which did not look abnormal to Bob as this sometimes occurs naturally owing to atmospheric conditions (during sunset, sunrise, fog). We remark that this type of detector usually survives tens of mW for a short time^{8,37}. Even if we had to use a wavelength within the BPF’s passband, detector exposure to higher power could likely be avoided by shaping Eve’s damaging beam.

After the damage, as the third step we replaced the damaging setup with the scanning setup again, and performed the final scanning of Bob’s receiver with the damaged pinhole. The results are shown in Fig. 3b. Now, the four receiver channels H, V, D, A exhibited unequal sensitivity to photons outside the middle area around $\phi = \theta = 0$. These efficiency plots were different from those measured in Ref. 16 without the pinhole, because of extra scattering at the edges of our laser-enlarged pinhole.

Predicted attack on free-space QKD system with damaged pinhole. We model a practical faked-state attack as described in Ref. 16. We assume a part of Eve is situated outside Alice and measures the quantum states coming out. Then, another part of her regenerates the measured quantum states as attenuated coherent pulses and sends them to Bob, tilting her beam at an angle such that it has a relatively higher probability of being detected by the desired detector. Eve has information about Bob’s receiver characteristics after the laser damage, and only uses devices available in today’s technology¹⁶. For example, let’s assume Eve sends a horizontally polarized light pulse. In this case, she should choose her tilt angle (ϕ, θ) from a subset \tilde{H} selected in such a way that the efficiency $\eta_h(\tilde{H})$ of Bob’s horizontal channel in \tilde{H} is as high as possible, in order to maximize mutual information Eve–Bob. On the other hand, if Bob measures in the opposite (DA) basis, the detection probabilities in the D and A channels $\eta_d(\tilde{H})$ and $\eta_a(\tilde{H})$ should be as low as possible, to minimize QBER. Thus, to find attack angles for the horizontally polarized light, we choose \tilde{H} that satisfies $\eta_h(\tilde{H}) \geq 0.6$ and

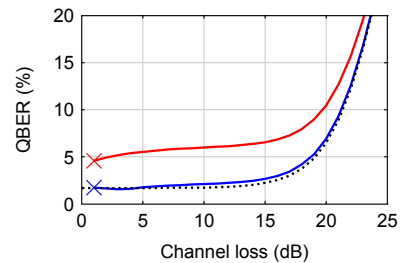


FIG. 5. **Modeled QBER observed by Bob in free-space QKD system.** The dotted curve shows QBER without Eve. At lower channel loss, the QBER is due to imperfect fidelity, while at higher channel loss Bob’s detector background counts become the dominant contribution. The lower solid curve (blue) shows QBER under our attack when only Bob’s sifted key rate is kept the same as before the attack. The upper solid curve (red) additionally keeps the same sifted key rates conditioned on each polarization sent by Alice, which more closely mimics a realistic system operation (see Ref. 16 for details).

$\delta(\tilde{H}) = \min \left\{ \frac{\eta_h(\tilde{H})}{\eta_d(\tilde{H})}, \frac{\eta_h(\tilde{H})}{\eta_a(\tilde{H})} \right\} \geq 100$. Similarly, for V, D and A polarized pulses, we choose attack angles that satisfy $\eta_v(\tilde{V}) \geq 0.03$, $\delta(\tilde{V}) \geq 4.5$; $\eta_d(\tilde{D}) \geq 0.6$, $\delta(\tilde{D}) \geq 120$; $\eta_a(\tilde{A}) \geq 0.2$, $\delta(\tilde{A}) \geq 22$. These subsets of angles are shown in the rightmost plot in Fig. 3b. Note that the thresholds η and δ used here are not optimal and have been picked manually. However, they satisfy the required conditions to successfully perform the faked-state attack with a resultant QBER $\leq 6.6\%$ in 1–15 dB channel loss range, as shown in Fig. 5. In the simulation, we assumed that Alice–Bob and Alice–Eve fidelity $F = 0.9831^{16,21}$, while Eve–Bob experimentally measured $F = 0.9904$. All other assumptions were the same as in Ref. 16.

Additional considerations in experiment on fiber-optic system. When we began testing the system components for laser damage, the synchronization detector D_{sync} initially presented an obstacle. This detector was based on an optical receiver module (Fujitsu FRM5W232BS) incorporating an avalanche photodiode biased below breakdown at > 30 V, providing an avalanche multiplication factor ≈ 6 . It only took about 6 mW of optical power at the photodiode (translating to about 0.15 W at Alice’s entrance) to die. It stopped providing the synchronization signal for Alice and thus broke the system. After an investigation, it turned out that the energy that killed it was chiefly provided by its high-voltage electrical bias circuit and not the optical signal. The bias circuit was based on a specialised integrated circuit with overcurrent protection (Maxim Integrated MAX1932ETC) followed by an LC low-pass filter with inductor $L = 330 \mu\text{H}$ and capacitor $C = 0.47 \mu\text{F}$. If the optical power is applied suddenly, with sub-nanosecond rise time, it momentarily induces a large photocurrent supplied from C that destroys the avalanche photodiode. If, however, the optical power is applied gradually, with millisecond rise time, C discharges slowly and then the relatively slow overcurrent protection reacts in the integrated circuit, lowers the bias voltage and saves the photodiode. We thus added a manual shutter to the EDFA to make the damaging power rise from zero slowly, allowing D_{sync} to easily withstand the optical power used in our attack while being electrically powered up. Another solution could be to damage the system when it is without electrical power. It can also be said that we could choose to selectively damage one of two components in Alice, albeit one of them bricking the system.

We ran our damage tests with VOA2 (OZ Optics DD-600-11-1300/1550-9/125-S-40-3S3S-1-1-485:1-5-MC/IIC) set at 2 dB, because this is what the manufacturer’s QKD software available for the research system Clavis2 set it at. The support of the pulse-energy-monitoring countermeasure was not implemented in this software²². In contrast, the manufacturer’s factory-calibration software supported it fully and set VOA2 between 2 and ≈ 15 dB, complementary to the channel loss, in order to maintain constant power at the three Alice’s detectors D_{pulse} , D_{sync} , and D_{cw} . The higher settings of VOA2 would require more laser power to damage D_{pulse} . However, D_{pulse} could also be damaged during the system start-up time, when it sends the homing command to VOA2. The homing command causes it to traverse its lowest attenuation values for a

few seconds, likely being sufficient for Eve to do the damage at already demonstrated power levels.

Supplementary Video 1. Real-time video recording of laser damage to the spatial filter inside Bob’s setup. Download the video at <http://vad1.com/pinhole-laser-damage-20140825.wmv> (Windows Media Video, 14.4 MiB) or <http://vad1.com/pinhole-laser-damage-20140825.ppsx> (PowerPoint Show, 17.0 MiB). The video shows the spatial filter (Thorlabs P20S) illuminated by 3.6 W c.w. 810 nm laser beam for 10 s, focused in a spot much wider than the original pinhole diameter of 20 μm . This is a filter sample with a slightly smaller original pinhole diameter than the one used to obtain efficiency mismatch data in this article and shown in Fig. 2b. The samples were otherwise of the same type and damaged under the same conditions. The video was taken via a mirror lowered inside Bob’s setup. The pinhole plane was imaged from the front side at an angle slightly off normal, in order for the mirror not to obstruct the damaging beam. Canon MP-E 65 mm lens was used at $2.8\times$ magnification and f/16 lens aperture (f/60 effective aperture), with Canon EOS 7D camera body. The pinhole was brightly lit sideways with a fiber-optic illuminator bundle, in order to bring up detail. During the laser exposure, the steel foil can be seen deforming from heat, popping out of focus and apparently shifting laterally in the image; however the lateral shift is an artefact of the camera’s angle of view being off-normal. After the laser is switched off, the foil cools and returns to the original position, now with about 150 μm diameter hole in it. Sound was added later for an artistic effect.